Supporting Information Appendix

Symbiotic polydnavirus and venom reveal parasitoid to its hyperparasitoids

Feng Zhu, Antonino Cusumano, Janneke Bloem, Berhane T. Weldegergis, Alexandre Villela, Nina E. Fatouros, Joop J.A. van Loon, Marcel Dicke, Jeffrey A. Harvey, Heiko Vogel, Erik H. Poelman

SI Text

The role of salivary glands in induction of plant volatiles by parasitized and unparasitized caterpillars

In total, 50 volatile compounds were tentatively identified across all five experimental plant treatments (undamaged, UD, plants damaged by intact unparasitized (S+) and parasitized (PS+) caterpillars as well as those ablated of their salivary glands (PS- and S-). Apart from the absence of (*E*)-2-butenenitrile in undamaged control plants, there were no other qualitative differences in the composition of volatile blends among treatments (Table S1). A multivariate analysis that included all sampled plant treatments resulted in a model with one significant principle component (Figure 2a; PLS-DA, $R^2X = 0.195$, $R^2Y = 0.13$, $Q^2 = 0.064$). In this model, a total of 19 compounds had VIP (variable importance in the projection) values > 1 (Table S1), which were the most important compounds that differentiated the volatile blends. These compounds include nine monoterpenes, two sesquiterpenes, two nitriles, two ketones, two esters, one alcohol, and one unknown compound (Table S1).

Pairwise comparison by PLS-DA for plant volatiles induced by mock-treated and ablated unparasitized *P. brassicae* revealed a model with one significant principle component (PLS-DA, $R^2X = 0.223$, $R^2Y = 0.408$, $Q^2 = 0.08$) (Fig. 2d). Among the 21 compounds that had VIP values > 1, three compounds showed higher emission by plants that were induced by mock-treated unparasitized caterpillars, which were 3-methylbutanenitrile, (*E*)-4,8-dimethyl-1,3,7-nonatriene (DMNT) and (*E*,*E*)-α-farnesene (Mann–Whitney *U* tests, P = 0.041, P = 0.041, and P = 0.049, respectively).

Pairwise comparison by PLS-DA for plant volatiles emitted by plants induced by mock-treated and ablated *C. glomerata*-parasitized *P. brassicae* did not result in a significant model when all ten samples for each treatment were included. Using PCA, one outlier sample from mock-treated parasitized caterpillar induced plants was visualized in the score plot. Upon

www.pnas.org/cgi/doi/10.1073/pnas.1717904115

removing this outlier, subsequent PLS-DA analyses revealed one significant principle component (PLS-DA, $R^2X = 0.256$, $R^2Y = 0.39$, $Q^2 = 0.051$). In this model, there were 22 compounds with VIP values > 1, including different terpenoids, nitriles, ketones, esters and one alcohol (Fig. 2c). Among these compounds, 6,10-dimethyl-2-undecanone and an unknown compound were emitted in higher amounts by plants induced by mock-treated *C. glomerata*-parasitized *P. brassicae* (Mann–Whitney *U* tests, P = 0.049, for both compounds). Moreover, two compounds, namely (*Z*)-3-hexen-1-ol and 1-methyl-4-(1-methylethyl) cyclohexanol, had a marginally significant increase in release by plants induced by mock-treated parasitized caterpillars (Mann–Whitney *U* tests, P = 0.059, for both compounds). In addition, the multivariate analysis did not differentiate volatile blends emitted by plants induced by ablated unparasitized or ablated parasitized *P. brassicae* caterpillars (Fig. 2b).

Differential gene expression in salivary glands of parasitized and unparasitized caterpillars

The *de novo* transcriptome assembly (TA) generated 24,054 contigs (N50 = 2432) that allowed more than 90% of the individual reads used for the combined assembly to be remapped. More than 98% of the total TA-contigs could be remapped with reads corresponding to samples from both caterpillar treatments (Table S2). We identified 7612 sequences (> 31%) matching entries in the GenBank nonredundant (NR) database with *E*-value cut-off = 10^{-5}, whereas 16,442 sequences (> 68%) did not yield matches.

The magnitude of differential transcription in labial salivary glands due to parasitism was visualized by comparing the number of contigs differentially expressed between unparasitized and *C. glomerata* parasitized *P. brassicae* caterpillars (Fig. 3a; Fig. S1). A total of 347 contigs were differentially expressed in labial salivary glands between unparasitized and parasitized caterpillars (false discovery rate, P < 0.05; fold change > 2). There were 237 contigs with higher expression in salivary glands extracted from parasitized caterpillars, whereas 110 contigs were expressed more strongly in salivary glands of unparasitized caterpillars (Table S3).

Gene ontology (GO) -enrichment analysis revealed that nutrient reservoir activity was over-represented in salivary glands of unparasitized caterpillars (Fig. S2). In contrast, the GO terms that were over-represented in salivary glands of *C. glomerata* parasitized caterpillars included modulation of host processes by viruses and virus suppression of host NF-kappa B transcription factor (Fig. S2). Interestingly, we found that the expression of genes encoding β-glucosidase as well as storage proteins involved in growth and development were suppressed

in salivary glands of parasitized caterpillars (Table S3). Some other proteins with suppression in salivary glands of parasitized caterpillars were cuticle proteins, e3 ubiquitin-protein ligase, distal antenna-like protein, and latrophilin-like receptor (Table S3). In contrast, glucose dehydrogenase, an enzyme contributing to suppression of plant defences, was up-regulated in salivary glands of parasitized caterpillars (Table S3). Some other genes up-regulated in salivary glands of parasitized caterpillars were those that code for Krueppel homologs, arylsulfatase B, trehalase and trehalose transporters, and β-fructofuranosidase (Table S3).

In conclusion, the up and down regulation of genes in salivary glands of parasitized caterpillars suggest that parasitism affects physiology of the herbivore broadly.

SI Methods

Microinjections of wasp-derived components into caterpillars, plant induction and hyperparasitoid preference tests for caterpillar induced plant volatiles.

Extracting polydnavirus particles (PDVs) and venom. Female *C. glomerata* wasps were anesthetized on ice and dissected in phosphate-buffered saline (PBS) under a light microscope. The ovaries containing calyx fluid with virus particles and the venom apparatus (gland and reservoir) were each collected and stored separately in 250 µl PCR tubes. The total volume was adjusted with PBS to reach the desired concentration in wasp equivalents (w.e.) (for example: venom apparatus from 30 wasps in 30µl of PBS for injection of 100nl containing 0.1 w.e./caterpillar) (9). Venom gland and calyx were disrupted by several passages through a 20 µl micropipette cone. Tubes containing the extracts were centrifuged for 5 min at 5000 rpm (venom) or for 1 min at 500 rpm (calyx fluid) to spin down the tissues and to purify the virus particles (9). It has been shown that purification of the virus by centrifugation has similar effects on caterpillar physiology as other purification techniques such as filtration or by using a gradient (31). Presence of PDV particles in calyx extracts was confirmed under an electron microscope Zeiss EM 10 CR at 80 kV. Supernatants containing the venom or calyx extracts were stored on ice and injected within 6 h into L2 *P. brassicae* caterpillars (as described below). For injections with a mixture of venom and calyx fluid, equal volumes of the two extracts, each at double the routine concentration, were mixed before injection experiments (see *microinjections and plant induction*).

Isolation of *Cotesia glomerata* eggs for injection. Second instar *P. brassicae* caterpillars were parasitized by *C. glomerata* as described in the section "parasitic wasps" and rapidly dissected in PBS to recover the mature eggs. The eggs were suspended in 30 µl of PBS in a 250 µl PCR tube, pelleted gently (5 seconds at 1000 rpm) and washed three times using 30 µl of PBS medium.

Microinjections and plant induction. PBS solutions with components retrieved from parasitoids were injected into L2 *P. brassicae* caterpillars anesthetized with CO_2 using the Nanoject II Auto-Nanoliter Injector (Drummond). In all experiments, 0.1 wasp equivalent of venom, calyx fluid with PDVs or a mixture of venom and calyx fluid (with or without eggs) dissolved in 100 nl were injected. Eggs that had been collected not longer than 6h earlier were injected as aliquots of PBS containing approximately 20-40 eggs/100 nl. We prepared seven different caterpillar treatments to test the effect of each of three component of parasitism

individually (eggs, PDVs, venom) and their synergistic effects in a full factorial design: 1) eggs; 2) PDVs; 3) venom; 4) eggs + PDVs; 5) eggs + venom; 6) PDVs + venom; 7) eggs + PDVs + venom. The last treatment represents a microinjection of the full restoration of a parasitism event. Two additional treatments were used as controls to test whether the microinjection treatment *per se* affected the interaction of the caterpillars with the food plant: 8) Unparasitized caterpillars injected with 100 nl of PBS representing a treatment that is assumed to be less attractive to hyperparasitoids and 9) *C. glomerata* parasitized caterpillars injected with PBS of which feeding-induced plant volatiles should be preferred over those by unparasitized PBS injected caterpillars. After microinjections, the caterpillars that recovered within 2h were introduced to and allowed to feed on new fresh *Brassica oleracea* var. *gemmifera* cv. Cyrus plants for 7-10 days until they reached the fifth instar. At this point, the nine different caterpillar treatments were used to induce *B. oleracea* "Kimmeridge" plants to obtain the nine corresponding plant treatments. Two caterpillars were inoculated on each individual plant and allowed to feed for 24 h after which they were used in two choice Y-tube experiments for hyperparasitoid preference of HIPVs.

Hyperparasitoid preference for herbivore induced plant volatiles. In our previous work, we have shown that *L. nana* prefers plant volatiles induced by unparasitized or parasitized caterpillars over undamaged plants, and that volatiles from plants damaged by parasitized caterpillars are preferred over those from plants damaged by unparasitized caterpillars in the lab as well as field (11, 12). Here, we tested hyperparasitoid preference for plants induced by each of eight treatments in which caterpillars were microinjected with a component of parasitism against a plant damaged by unparasitized caterpillars injected with PBS. We addressed which component of parasitism or combination of components was needed to reach preference for the parasitized caterpillar-induced plant volatiles over volatiles induced by unparasitized control caterpillars. The Y-tube olfactometer assays followed the procedures described in Zhu et al. (2015) (12). We removed caterpillars and their feces from the plants and placed the plants in one of two glass jars (30 l each) that were connected to the two olfactometer arms. A charcoal-filtered airflow (4 l/min) was led through each arm of the Y-tube olfactometer system and a single wasp was released at the base of the stem section (3.5 cm diameter, 22 cm length) in each test (32). Wasps that reached the end of one of the olfactometer arms within 10 min and stayed there for at least 10 s were considered to have chosen the odor source connected to that olfactometer arm. We swapped the jars containing the plants after testing five wasps, to compensate for unforeseen asymmetry in the setup. Each

set of plants was tested for 10 wasps, and nine sets of plants for each treatment combination were tested. After each set of plants was tested, the glass jars were cleaned using distilled water and dried with tissue paper. The Y-tube olfactometer set-up was placed in a climatized room, and in addition to daylight, it was illuminated with four fluorescent tubes (FTD 32 W/84 HF, Pope, The Netherlands).

Statistical analysis. Two-tailed binomial tests were applied to each treatment pair, we used a GLM and post-hoc LSD test to compare binomial choice distributions among the two-choice experiments. All tests were performed with the statistical software package IBM SPSS Statistics 19 (SPSS Inc., Chicago, IL, USA).

Surgical removal of caterpillar salivary gland, plant induction and hyperparasitoid preference tests for caterpillar induced plants.

Surgical removal of caterpillar salivary gland. Ablation of labial salivary glands was performed on both unparasitized and *C. glomerata*-parasitized *P. brassicae* caterpillars when they reached the second day of their fifth larval instar and followed methods described in Musser et al. (2006) (24). In brief, the selected unparasitized and parasitized caterpillars were contained in separate 7-inch diameter Petri dishes and sedated by chilling on ice for 15 min. Then, a single caterpillar was transferred to a dissection plate that was filled with an ice-cold autoclaved solution of PBS. While the caterpillar was submerged in the PBS solution, the second abdominal segment between the true legs and prolegs was held from the dorsal side of the caterpillar using forceps. Subsequently, a miniscule incision was made in the cuticle revealing the pair of labial salivary glands. With a forceps, the complete labial salivary glands were gently removed from the body cavity. For parasitized caterpillars, larvae of *C. glomerata* occasionally emerged from the incision. Therefore, only those caterpillars that had no more than three out of a brood size of 15-30 parasitoid larvae slipping out of the incision were included in the study. After the ablation of the salivary glands, the caterpillar was carefully rinsed with distilled water, dried with tissue paper and transferred to a new Petri dish supplied with a fresh *B. oleracea* leaf. The caterpillar was allowed to recover from the surgery in the Petri dish for three hours. Caterpillars that within these three hours started feeding on the plant leaf were selected for subsequent plant induction. Mock-treated unparasitized and parasitized caterpillars were subjected to the same protocol, including the incision, but the labial salivary glands were not removed from the body cavity of the caterpillar. To ensure that ablated caterpillars fed similar amounts of leaf tissue as mock treated caterpillars, we

quantified the amount of leaf damage for 10 plants for each herbivore induction treatment, using a transparent plastic sheet with 1 mm^2 grid. We did not find apparent reduction in food consumption of ablated caterpillars compared to mock-treated caterpillars (Student's t-tests; for unparasitized caterpillars, t = 1.197, df = 18, P = 0.471; for parasitized caterpillars, t = 1.202, df = 18, P = 0.118). After the experiments, the ablated unparasitized caterpillars successfully pupated and eclosed as adult butterflies. For ablated parasitized caterpillars, fully grown parasitoid larvae eventually emerged and pupated.

Plant treatments and hyperparasitoid preference tests. We offered female hyperparasitoids (*L. nana*) two-choice tests for combinations of five plant induction treatments in a Y-tube olfactometer setup as described by Takabayashi and Dicke (1992) (32). The wild *B. oleracea* plants were treated with two fifth-instar caterpillars for 24 hours: 1) *P. brassicae* caterpillars with intact labial salivary glands (S+); 2) *P. brassicae* caterpillars with ablated labial salivary glands (S-); 3) *C. glomerata* parasitized *P. brassicae* caterpillars with intact labial salivary glands (PS+); 4) *C. glomerata* parasitized *P. brassicae* caterpillars with ablated labial salivary glands (PS-); or 5) plants were left untreated serving as the undamaged control (UD). In our previous work, we have shown that *L. nana* prefers plant volatiles induced by unparasitized and parasitized caterpillars over undamaged plants, and that volatiles from plants damaged by parasitized caterpillars are preferred over those from plants damaged by unparasitized caterpillars (12). For clarity of the results obtained in the current study, we included these results as reference in Figure 1b. In the current study, we tested whether the labial salivary gland plays a crucial role in differential induction of plant responses and whether ablation of the glands eliminates the hyperparasitoid preference for plant volatiles induced by parasitized caterpillars over unparasitized caterpillars. We first offered *L. nana* plant volatiles induced by either unparasitized or parasitized *P. brassicae*, both ablated of labial salivary glands to test whether this hyperparasitoid could still discriminate volatile blends resulting from these treatments. Subsequently, we tested *L. nana* attraction to plant volatiles induced by mock-treated caterpillars versus volatiles induced by caterpillars from which the labial salivary glands had been ablated within the same category (unparasitized or parasitized). Finally, we tested preferences of *L. nana* for plant volatiles released by undamaged control plants versus plant volatiles induced by unparasitized or parasitized *P. brassicae* caterpillars with the labial salivary glands ablated, to test whether hyperparasitoids respond to plant volatiles induced by caterpillars without labial salivary glands. For each pairwise comparison, 70 *L. nana* females

were tested. The Y-tube olfactometer assays followed the procedures described in the choice tests with microinjected caterpillars.

Statistical analysis: Two-tailed binomial tests were applied to each treatment pair, using the statistical software package IBM SPSS Statistics 19 (SPSS Inc., Chicago, IL, USA).

Plant volatile collection and analysis.

Volatile collection. To characterize the *B. oleracea* plant volatiles induced by parasitized and unparasitized caterpillars as well as the effect of labial saliva of *P. brassicae* on emission of HIPVs, we collected headspace samples of 10 replicate plants for each of five plant treatments. In each of these treatments, herbivores were allowed to feed for 24 h following the methods of the Y-tube hyperparasitoid preference tests: 1) *P. brassicae* caterpillars with intact labial salivary glands (S+); 2) *P. brassicae* caterpillars ablated of labial salivary glands (S-); 3) *C. glomerata*-parasitized *P. brassicae* caterpillars with intact labial salivary glands (PS+); 4) *C. glomerata*-parasitized *P. brassicae* caterpillars ablated of labial salivary glands (PS-); or 5) plants were left untreated serving as the undamaged control (UD). The subsequent plant volatile collections followed procedures described in Zhu et al. (2015) (12). In short, just before volatile collections, we removed the caterpillars and their frass from plants. Dynamic headspace sampling was carried out in a climate room, using five-week-old potted plants. Pots were carefully wrapped in aluminum foil to minimize odor contribution from pots and/or soil. During volatile collection, the plants were placed individually into a 30-l glass jar, which was sealed with a viton-lined glass lid with an inlet and outlet. Compressed air was filtered by passing through charcoal before reaching the glass jar containing the plant. Volatiles were collected by sucking air out of the glass jar at a rate of 200 ml/min through a stainless steel tube filled with 200 mg Tenax TA (20/35 mesh; CAMSCO, Houston, TX, USA) for 2h (12).

Volatile analysis. Thermo Trace GC Ultra in combination with Thermo Trace DSQ quadrupole mass spectrometer (Thermo Fisher Scientific, Waltham, USA) was used for separation and detection of plant volatiles. Prior to releasing of the volatiles, each sample was dry-purged under a flow of nitrogen (50 ml/min) for 10 min at ambient temperature in order to remove moisture. The collected volatiles were then thermally released from the Tenax TA adsorbent using an Ultra 50:50 thermal desorption unit (Markes, Llantrisant, UK) at 250 °C for 10 min under a helium flow of 20 ml/min, while re-collecting the volatiles in a thermally cooled universal solvent trap: Unity (Markes) at 0 °C. Once the desorption process was

completed, volatile compounds were released from the cold trap by ballistic heating at 40 °C/s to 280 °C, which was then kept for 10 min, while the volatiles transferred to a ZB-5MSi analytical column [30 m x 0.25 mm I.D. x 0.25 μm F.T. with 5 m built in guard column (Phenomenex, Torrance, CA, USA)], in a splitless mode for further separation. The GC oven temperature was initially held at 40 °C for 2 min and was immediately raised at 6 °C/min to a final temperature of 280 °C, where it was kept for 4 min under a helium flow of 1 ml/min in a constant flow mode. The DSQ mass spectrometer (MS) was operated in a scan mode with a mass range of 35 – 400 amu at 4.70 scans/s and spectra were recorded in electron impact ionisation (EI) mode at 70 eV. MS transfer line and ion source were set at 275 and 250 °C, respectively. Tentative identification of compounds was based on comparison of mass spectra with those in the NIST 2005 and Wageningen Mass Spectral Database of Natural Products MS libraries, in combination with experimentally obtained linear retention indices (LRI). We used peak area of each compound in the chromatogram for compound quantification (12).
Statistical analysis. The differences in composition of the volatile headspaces of the five plant treatments were analyzed using principal component analysis (PCA) and projection to latent structures–discriminant analysis (PLS-DA; PCA and PLS-DA modules of SIMCA-P 12.0.1, Umetrics, Umeå, Sweden). The measured peak areas for the volatile blends in the different treatments were log-transformed, mean-centered and scaled to unit variance before being analyzed using PCA and PLS-DA. The results of the PLS-DA analysis are visualized in score plots. The score plots reveal the sample structure according to the model components. Volatile compounds that were identified to contribute strongly to differences among treatments as indicated by Variable Importance in the Projection (VIP) values larger than 1, were subjected to Mann-Whitney U-tests to test the statistical differences between individual treatments (12).

RNA-seq and transcriptome analyses.

Labial salivary glands extraction and RNA isolation. To study the labial salivary gland tissue-specific transcriptional differences of genes in unparasitized and *C. glomerata* parasitized caterpillars, labial salivary glands of the two types of caterpillars were extracted following the ablation procedure described above (Surgical removal of caterpillar salivary gland). We pooled 15 pairs of labial salivary glands per sample, collecting four biological replicates of the two treatments. After extraction, samples were immediately flash-frozen in liquid nitrogen. Total RNA was extracted from each of the labial salivary gland samples (4 samples from unparasitized *P. brassicae* and 4 samples from *C. glomerata* parasitized *P. brassicae*

larvae) using the innuPREP RNA Mini Isolation Kit (Analytik Jena, Jena, Germany) following the manufacturers' guidelines. The integrity of the RNA was verified using an Agilent 2100 Bioanalyzer and a RNA 6000 Nano Kit (Agilent Technologies, Palo Alto, CA). The quantity as well as OD 260/280 and 260/230 ratios of the isolated RNA samples were determined using a Nanodrop ND-1000 spectrophotometer.

Illumina sequencing and transcriptome assembly. Tissue-specific transcriptome sequencing of eight RNA pools was carried out on an Illumina HiSeq2500 Genome Analyzer platform using paired end (2 x 100 bp) read technology with RNA fragmented to an average of 150 nucleotides. Library construction and sequencing was performed by the Max Planck Genome Center Cologne, Germany (http://mpgc.mpipz.mpg.de/home/). 1 µg of total RNA each was used for generating TruSeq RNA libraries and mRNA enrichment was performed. Approximately 40 million reads per biological replicate and per treatment were obtained. Quality control measures, including filtering high-quality reads based on the score given in fastq files, removing reads containing primer/adaptor sequences and trimming read length were carried out using CLC Genomics Workbench v7.1 (http://www.clcbio.com). The *de novo* transcriptome assembly (TA) was carried out using CLC Genomics Workbench software v7.1 (http://www.clcbio.com) by comparing an assembly with standard settings and two additional CLC-based assemblies with different parameters, selecting the presumed optimal consensus transcriptome according to published details (33). Any conflicts among the individual bases were resolved by voting for the base with highest frequency. Contigs shorter than 200 bp were removed from the final analysis. The resulting final *de novo* reference TA (backbone) contained 24,054 contigs with a N50 contig size of 2432 bp and a maximum contig length of 22092 bp.

Homology searches and annotation. BLASTx and BLASTn homology searches with our contig sequences were conducted on a local server using the National Center for Biotechnology Information (NCBI) blastall program. First, sequences were searched against the NCBI NR protein database using an E-value cut-off of 10^{-3} to find predicted polypeptides with a minimum length of 15 amino acids. Second, sequences with no BLASTx hits were used as queries in a BLASTn search against an NCBI NR nucleotide database with an E-value cut-off of 10^{-10}. Blast results were imported as xml files and further processed using the BLAST2GO-PRO software suite (www.blast2go.de) (34). Functional annotations were assigned to the *P. brassicae* TA contigs using a sequential strategy based on gene ontology (GO) terms (www.geneontology.org), InterPro terms (InterProScan, EBI), enzyme

classification (EC) codes and KEGG metabolic pathways (Kyoto Encyclopedia of Genes and Genomes). Enzyme classification codes and KEGG metabolic pathway annotations were generated from the direct mapping of GO terms to their enzyme code equivalents. Finally, InterPro searches were carried out remotely against the InterProEBI web server. Enrichment analyses were carried out by comparing the GO-annotations from each differentially expressed contig subset (test sets) with the complete TA contig set (reference set) by running a two-tailed Fisher's exact test using the appropriate Blast2GO web application (http://www.blast2go.com/webstart/makeJnlp.php) with false discovery rate (FDR) correction for multiple testing and a P-value of 0.05. The Blast2GO web application was configured to access the local GO database previously used to assign GO terms.

Digital gene expression analysis. Digital gene expression analysis was carried out by using QSeq Software (DNAStar Inc.) to remap the Illumina reads from all eight samples onto the reference backbone and then counting the sequences to estimate expression levels using previously described parameters for read mapping and normalization (33). For read mapping, we used the following parameters: n-mer length = 25; read assignment quality options required at least 25 bases (the amount of mappable sequence as a criterion for inclusion) and at least 90% of bases matching (minimum similarity fraction, defining the degree of preciseness requires) within each read to be assigned to a specific contig; maximum number of hits for a read (reads matching a greater number of distinct places than this number are excluded) = 10; n-mer repeat settings were automatically determined and other settings were not changed. Biases in the sequence datasets and different transcript sizes were corrected using the RPKM algorithm (reads per kilobase of transcript per million mapped reads) to obtain correct estimates for relative expression levels. To control for the effect of global normalization using the RPKM method, we also analyzed a number of highly conserved housekeeping genes frequently used as control genes in qPCR analysis. These controls included several genes encoding ribosomal proteins (rpl3, rpl5, rpl7a, rps3a, rps5, rps8, rps18 and rps24), elongation factor 1alpha and eukaryotic translation initiation factors 4 and 5. The corresponding genes were inspected for overall expression levels across samples and were found to display expression level differences (based on RPKM values) lower than 1.3-fold between samples, indicating they were not differentially expressed and validating them as housekeeping genes. Hierarchical clustering was performed with the QSeq software using the Euclidean distance metric and using the Centroid Linkage method.

β-glucosidase activity in labial salivary gland.

Sample preparation. To measure the β-glucosidase activity in labial salivary glands (lsg) of parasitized and unparasitized caterpillars, lsg were extracted following the ablation procedure described above (Surgical removal of caterpillar salivary gland). The other caterpillar treatments were micro-injection of parasitoid eggs, venom, calyx fluid containing polydnaviruses (PDVs), and combinations of these, in phosphate-buffered saline (PBS) solution (prepared from tablets; Oxoid). In 1.5 ml safe-lock tubes (Biosphere safe seal, Sartstedt), lsg of 3 or 15 caterpillars (unmanipulated caterpillars or micro-injected caterpillars respectively) were pooled into one sample. We prepared 25 samples for the comparison between unparasitized and parasitized caterpillars, 10 replicates were prepared for each of the micro-injection treatments. Samples were firstly kept on ice and, then, stored at −80 °C. Once resuming the sample preparation, samples were sonicated for cell disruption using a Digital Sonifier (102C, Branson) in two intervals of 10 s, with the intensity set to 5%. Samples were kept on ice during sonication to reduce damage to proteins by overheating. The sonication step was followed by centrifugation for 10 min at 10 000 g (Centrifuge 5430, Eppendorf). Supernatants were transferred to clean 1.5 ml safe-lock tubes, and stored at −80 °C until use. The protocol for measuring β-glucosidase activity was based on the papers by Mattiacci *et al.* (1995), Pankoke *et al.* (2012) and Reed *et al.* (2003) (16, 35, 36) (*SI Text* for detailed protocol). The number of salivary glands pooled for the comparison of β-glucosidase activity in salivary glands of parasitized versus unparasitized caterpillar (n = 3) differed from the number pooled for caterpillars with different micro-injection treatments (n = 15). We pooled more salivary glands for the micro-injected caterpillars, because of the expected larger variation in response of the caterpillars and the success of establishment of the micro-injection treatments. Thereby, the enzyme activity values differ between the two caterpillar groups and were analysed with two separate statistical models. We use an ANOVA with fixed factor of treatment (parasitized / unparasitized or one of six micro-injection treatments) and a co-variate of total protein concentration to account for the lower total protein concentration found in parasitized caterpillars.

Protocol for measurement of β-glucosidase activity

β-glucosidase activity was determined by exposing the substrate 4-nitrophenyl β-D-glucopyranoside (nitrophenyl glucoside, **npg**) to **lsg** samples for 2 hours. In the reaction, the glucose moiety of **npg** is cleaved off by β-glucosidase, with 4-nitrophenol being formed. As

the UV–vis absorption spectrum of deprotonated 4-nitrophenol (4-nitrophenolate ion, **npl**) is different from that of **npg**, with **npl** having a much larger molar absorptivity at 400 nm than **npg**, the concentration of **npl** formed is obtained from the absorbance reading at that wavelength. The following was added to 1.5 ml safe-lock tubes: 220 µl of 0.01 M citrate buffer pH 6 solution (prepared as described below), 20 µl of **npg** solution (prepared as described below), and 10 µl of **lsg** sample. The resulting concentration of **npg** was 2.0 mM. This was followed by placement of the tubes in an incubator shaker (ThermoMixer F1.5, Eppendorf) for 2 h at 30 °C, 800 rpm. The reaction was quenched by removing the tubes from the incubator shaker, and adding 500 µl of 0.5 M sodium carbonate solution (prepared as described below). The resulting solutions were transferred to 10 mm optical-path disposable cuvettes (Semi-micro cuvettes, Greiner Bio-One), followed by measurement of the absorbance at 400 nm in a Smartspec 3000 spectrophotometer (BioRad). Analyses of control-samples were carried out together with every sequence of samples. Such samples were analysed as described in this section, with the following differences:

- No **npg** solution (0.01 M citrate buffer pH 6 solution instead); for subtracting the contribution to the absorbance at 400 nm of **lsg** samples from that of **npl**. This was done once per sample, in each sequence of samples.
- No **lsg** sample (0.01 M citrate buffer pH 6 solution instead); for subtracting the contribution to the absorbance at 400 nm of **npg**, and **npl** present due to its auto-hydrolysis, from that of **npl** present due to hydrolysis of **npg** via β-glucosidase's action. In each sequence of samples, n = 2 or 3.

Notes:

- The (lamp of the) spectrophotometer was warmed up for at least 30 min before measurements.
- The absorbance reading of the spectrophotometer at 400 nm was set to zero with 0.01 M citrate buffer pH 6 solution–0.5 M sodium carbonate solution 1:2 in a disposable cuvette. Then, the absorbance of this solvent mixture–cuvette was measured once or twice in each sequence of samples.
- Samples in this section refer to technical replicates of a biological replicate of a caterpillar treatment. The number of samples of biological replicates of caterpillar treatments was either 2 or 4 (with exceptions being 3 in one case, and 1 in another).

Calculations. Enzyme activity under the reaction conditions of samples was determined from the absorbance measurements at 400 nm. Absorbance values used for the calculations were obtained as follows:

Absorbance value used = $\text{absorbance}_{\text{sample}}$* − $\text{absorbance}_{\text{control–samples}}$** − $\text{absorbance}_{\text{solvent mixture–cuvette}}$***

Typically, data of 1:5 or 1:10 dilutions were used whenever the absorbance values of undiluted solutions were above 1.000 AU. In all samples conversion of **npg** was ≤ 10 – 11% (with exceptions being the samples of one biological replicate of a caterpillar treatment, in which the conversion of **npg** was 13 – 14%). This is important as, in such a way, **npg** was present in large excess relative to β-glucosidase throughout the reaction and the reaction is expected to have proceeded at its initial (maximum) rate (35). Concentrations of **npl** were determined from the absorbance values, using the molar absorptivity of **npl** at 400 nm (determined as described below). Amounts of **npl** present due to hydrolysis of **npg** via β-glucosidase's action (in nmol) were calculated after correcting for the dilution due to the addition of the 500 µl of 0.5 M sodium carbonate solution. Because these amounts are the same as those of **npg** (substrate) converted, enzyme activity values (in nmol min^{-1}) were obtained dividing them by 120 (min, as the reaction time was precisely 2 h). Notes:

- * n = 2 or 3 (few cases, n = 1); median used.
- ** In the case of control "no **lsg** sample", average used.
- *** Median was used in cases in which n = 2.
- This way of calculating the amount of **npl** present due to hydrolysis of **npg** via β-glucosidase's action is likely to entail an error. This is because the contribution to the absorbance of unreacted **npg**, and **npl** present due to auto-hydrolysis of **npg**, is subtracted from the $\text{absorbance}_{\text{sample}}$ value. During the analyses of the samples, however, part of **npg** is hydrolysed to **npl** via β-glucosidase's action. This is expected to diminish the absorbance due to unreacted **npg** (and possibly due to **npl** present due to auto-hydrolysis of **npg** too). Therefore, it is likely that the value which is subtracted from the $\text{absorbance}_{\text{sample}}$ values is larger than it should have been. Nonetheless, if this error is indeed present, it should be small as only 10–11% (or less) of **npg** were hydrolysed via the β-glucosidase's action and, thus, safe to neglect.

Procedure for the preparation of 0.01 M citrate buffer pH 6 solution, 0.5 M sodium carbonate solution, and solutions of 4-nitrophenyl β-D-glucopyranoside. The procedure for preparing the 0.01 M citrate buffer pH 6 solution was essentially that published online by Phillips [Phillips, T. How to Make Sodium Citrate Buffer. Accessed via https://www.thebalance.com/how-to-make-sodium-citrate-buffer-375494]. Hundred millilitres of 0.1 M stock solutions of citric acid (99%, Sigma-Aldrich; 21 g l^{-1}) and trisodium citrate dihydrate (99%, Merck; 29 g l^{-1}) were prepared using deionised water (prepared via a Reference A+ Millipore device, Merck). Fifty millilitres of 0.01 M citrate buffer pH 6 solution were prepared by adding 4.1 ml of stock solution of citric acid and 0.9 ml of stock solution of trisodium citrate dihydrate to 40 ml of deionised water. Then, the pH was adjusted with a sodium hydroxide (99%, Merck) solution. Finally, more deionised water was added, leading to the volume of 50 ml.

Notes:

- It was observed that the buffer solution becomes turbid over time. A good practice is, therefore, to use it while ≤ 5 days old.
- Mattiacci *et al.* (1995) and Pankoke *et al.* (2012) (16, 35) measured β-glucosidase activity using 0.1 M buffer solutions; that used by Pankoke *et al.* (2012) (35) was a sodium citrate–phosphate buffer pH 6.5. Using a scaled-up version of procedure now being reported and two different **lsg** samples, the change in pH before and after the 2 h incubation (30 °C, 800 rpm) period was observed to be only 0.1. Thus, the 0.01 M buffer solution used in this work is expected to have held the pH constant throughout the enzymatic reaction.

Two hundred millilitres of 0.5 M sodium carbonate (99.5-100.5%, Merck) solution were prepared using 10 g of sodium carbonate and deionised water. Solutions of **npg** (98%, Sigma-Aldrich; 7.5 mg mL^{-1}) were prepared using the 0.01 M citrate buffer pH 6 solution, in 5 mL volumetric flasks. **Npg** solutions were stored at −20 °C.

Procedure for the determination of the molar absorptivity of the 4-nitrophenolate ion at 400 nm. Primary stock solutions of 4-nitrophenol (100%, Sigma-Aldrich; 11.2 mg ml^{-1}) were prepared using the 0.01 M citrate buffer pH 6 solution, in 5 mL volumetric flasks. Secondary stock solutions and working solutions of 4-nitrophenol were prepared by two successive 10x-dilution steps, also using the 0.01 M citrate buffer pH 6 solution, in 5 ml volumetric flasks.

The following was added to 1.5 ml safe-lock tubes: 225 µl of 0.01 M citrate buffer pH 6 solution, 25 µl of 4-nitrophenol working solution, and 500 µl of 0.5 M sodium carbonate solution.* This was also done with 12.5 and 50 µl of 4-nitrophenol working solution, with the volume of the 0.01 M citrate buffer pH 6 solution added to the safe-lock tubes being adjusted accordingly (so that, together, the volumes of both solutions would amount to 250 µl). The resulting solutions were transferred to 10 mm optical-path disposable cuvettes, followed by measurement of the absorbance at 400 nm. This procedure was carried out three times for each of the volumes of 4-nitrophenol working solution (12.5, 25, and 50 µl). Thus, in total, nine solutions were analysed spectrophotometrically.** The molar absorptivity of **npl** at 400 nm ($\varepsilon_{\mathbf{npl},400}$) was calculated using the Beer–Lambert law, $\varepsilon = A\,c^{-1}$, as the path length (l) is 1 cm, and in which ε is the molar absorptivity, A is the measured absorbance of the solution, and c is the concentration of **npl**. The determination of the $\varepsilon_{\mathbf{npl},400}$ was carried out in duplicate, with the 4-nitrophenol stock and working solutions being prepared anew for the second determination. The determined $\varepsilon_{\mathbf{npl},400}$ values were 19 329 and 19 256 l mol^{-1} cm^{-1} (in each case, average of nine values). The $\varepsilon_{\mathbf{npl},400}$ value used for the calculations of enzyme activity (described above) was the average of these two experimentally determined values, *i.e.*, 19 293 l mol^{-1} cm^{-1}.

Notes:

- * Due to the basicity of the resulting solution (pH above 10), being the pK_a of 4-nitrophenol 7.15 [National Center for Biotechnology Information. PubChem Compound Database; CID=980, https://pubchem.ncbi.nlm.nih.gov/compound/980 (accessed Apr. 25, 2017)], 4-nitrophenol was present in solution as the 4-nitrophenolate ion.
- ** Such concentrations led to absorbance values <1.060 AU.

Supplementary figures

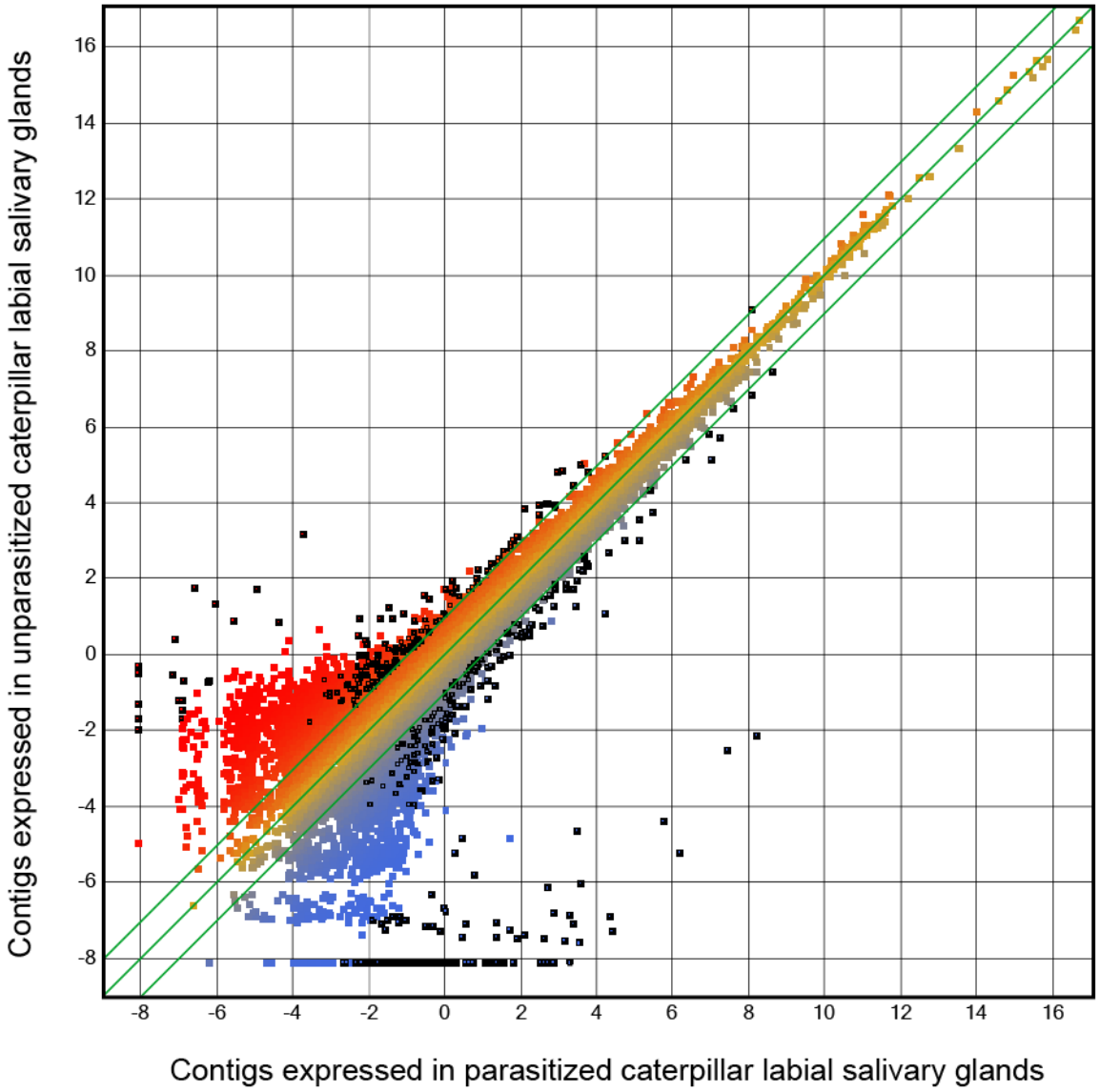

Fig. S1. Scatter plot showing global gene expression in labial salivary glands of *Pieris brassicae* isolated from unparasitized (Y-axis) or *Cotesia glomerata* parasitized (X-axis) caterpillars. Shown are $\log^2$ transformed RPKM values. Color indicates expression ratios of contigs that fall within a 2-fold cutoff. Contigs with expression ratios greater than 2-fold are shown in red (associated with labial salivary glands of unparasitized *P. brassicae*) or in blue (associated with labial salivary glands of parasitized *P. brassicae*). Contigs with expression ratios greater than 2-fold and $P < 0.05$ (FDA) are shown in black.

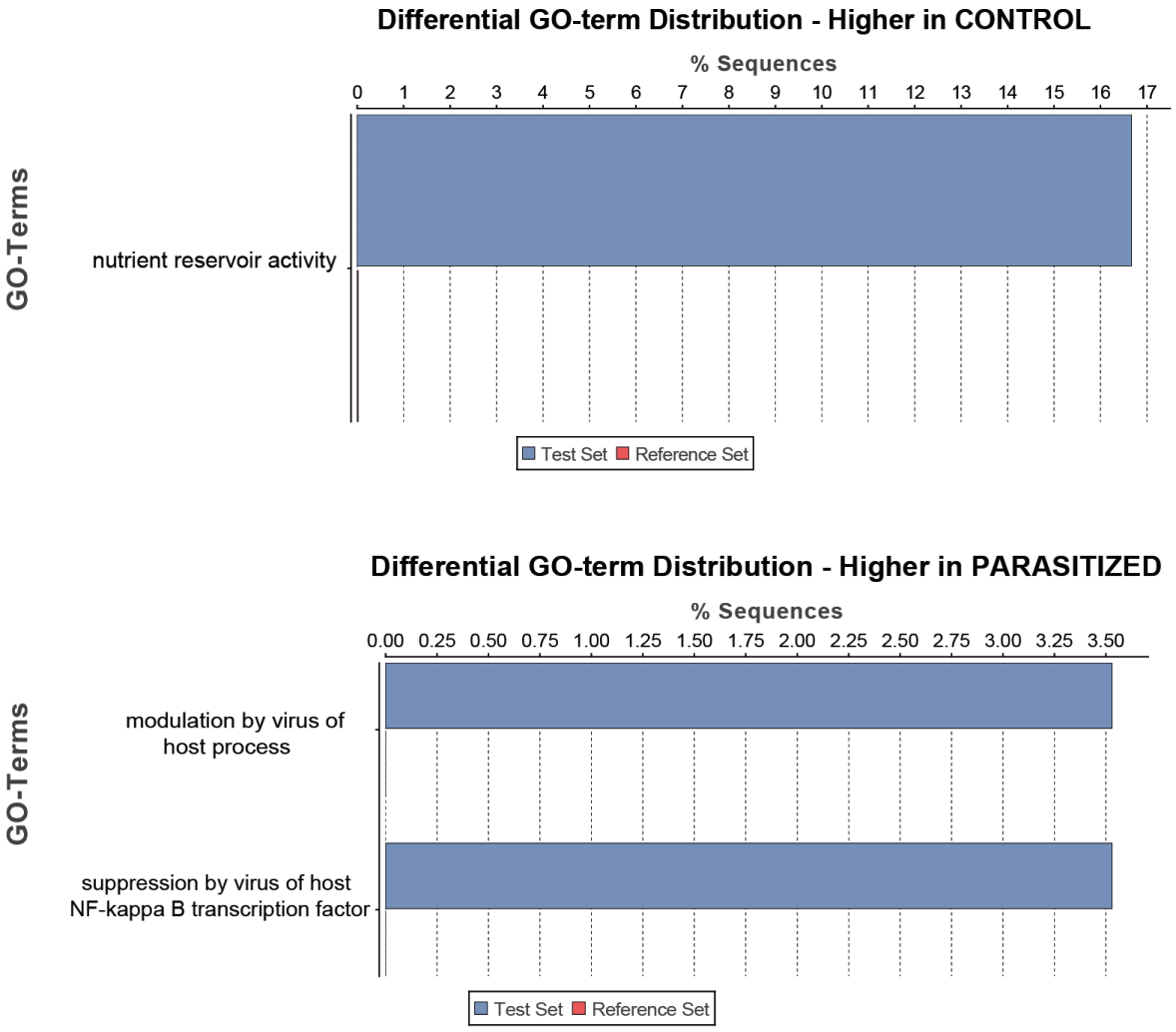

Fig. S2. Gene ontology (GO)-enrichment analysis for contigs with up-regulation in labial salivary glands of either unparasitized *Pieris brassicae* caterpillar (upper panel) or *Cotesia glomerata* parasitized caterpillars (lower panel).

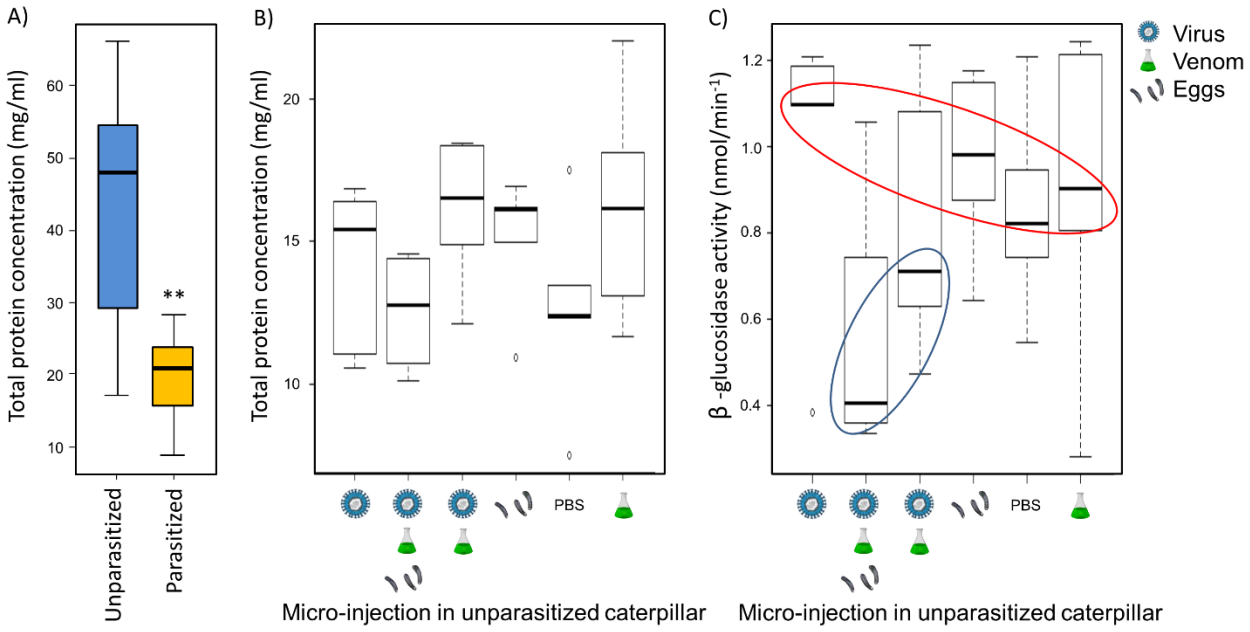

Fig. S3. Total protein concentration and β-glucosidase activity in salivary glands of *Pieris brassicae* caterpillars treated with parasitism or micro-injection with components of parasitism. (A) Total protein concentration in unparasitized (blue) or parsitized caterpillars (orange). Protein concentration is significantly lower in parasitized caterpillars (ANOVA on β-glucosidase activity (Fig. 3B) with total protein concentration as co-variate; total protein: $F = 128.236$, $P < 0.001$). (B) Total protein concentration in salivary glands of caterpillars treated with micro-injection of eggs, venom, PDV or a combination and compared to a mock-treated unparasitized caterpillar injected with PBS. Protein concentration is significantly dependent on micro-injection treatment (ANOVA on β -glucosidase activity (Fig. S3C) with total protein concentration as co-variate; total protein: $F = 66.321$, $P < 0.001$). (C) β-glucosidase activity in salivary glands of micro-injected caterpillars. Caterpillars injected with venom and PDV have lower β-glucosidase activity than caterpillars injected with PBS or single components of parasitism (ANOVA on β-glucosidase activity with total protein concentration as co-variate; β-glucosidase activity: $F = 5.679$, $P < 0.05$).

Table S1. Volatile compounds tentatively identified in the headspace of wild *Brassica oleracea* 'Kimmeridge' plants. Volatile emissions are given as mean peak area (SE) per gram fresh weight of plant divided by 10^4. Variable importance in the projection (VIP) values for the projection to latent structures–discriminant analysis are given. VIP values larger than 1 are shown boldfaced. Differences among treatments for compounds based on Mann–Whitney U pairwise comparisons are indicated with superscript letters.

No.	Compound	Class	UD^x (n = 10)	S-^{x} (n = 10)	S+^{x} (n = 10)	PS-^{x} (n = 10)	PS+^{x} (n = 10)	VIP score
1	(*E*)-2-butenenitrile	Nitrile	-^{a}	22.9 (6.5)^b	61.8 (22.3)^b	22.9 (7.2)^b	85.6 (37.9)^b	**3.20**
2	1-penten-3-ol	Alcohol	19.3 (6.7)^a	78.1 (26.1)^{ab}	215.2 (99.0)^b	26.8 (8.3)^a	80.6 (37.4)^{ab}	**1.19**
3	3-pentanone	Ketone	6.5 (1.5)^a	10.9 (3.1)^{ab}	32.5 (7.4)^b	8.9 (2.3)^a	23.8 (12.6)^{ab}	**1.21**
4	2-methylbutanenitrile	Nitrile	50.5 (16.8)^a	408.5 (170.9)^b	324.6 (198.8)^{ab}	600.1 (207.3)^b	1219.3 (717.2)^b	**1.17**
5	3-methylbutanenitrile	Nitrile	21.9 (3.6)	56.5 (11.3)	35.7 (12.0)	70.5 (27.2)	227.2 (159.2)	0.82
6	3-methyl-2-pentanone	Ketone	15.7 (3.2)^a	101.3 (35.4)^b	119.3 (35.0)^b	53.1 (9.0)^b	117.7 (36.2)^b	**2.23**
7	2,4-pentanedione	Ketone	16.6 (5.5)	6.5 (1.4)	15.4 (6.1)	5.2 (1.1)	7.5 (2.2)	0.63
8	(*Z*)-3-hexen-1-ol	Alcohol	36.0 (6.6)	136.2 (65.7)	379.3 (157.0)	41.1 (14.7)	275.1 (117.9)	0.58
9	(*Z*)-2-penten-1-ol, acetate	Ester	4.1 (1.6)	17.0 (6.9)	53.9 (20.1)	6.6 (2.7)	16.4 (9.2)	0.64
10	α-thujene	Monoterpene	155.9 (55.6)^a	274.8 (64.5)^{ab}	406.5 (70.7)^b	258.1 (39.9)^{ab}	334.5 (80.5)^{ab}	**1.08**
11	butylisothiocyanate	Ester	1.0 (0.5)	12.5 (5.5)	8.7 (4.8)	31.6 (14.7)	59.7 (40.1)	0.94
12	α-pinene	Monoterpene	99.4 (19.5)^a	132.2 (21.8)^{ab}	161.5 (22.0)^b	120.3 (13.6)^{ab}	161.6 (30.5)^{ab}	**1.05**
13	sabinene	Monoterpene	28.7 (10.1)^a	51.8 (12.0)^{ab}	75.6 (13.5)^b	47.4 (9.1)^{ab}	59.7 (13.2)^{ab}	**1.07**
14	β-pinene	Monoterpene	8.0 (2.0)^a	12.6 (2.5)^{ab}	17.8 (2.4)^b	12.0 (1.7)^{ab}	16.4 (3.0)^b	**1.45**
15	β-myrcene	Monoterpene	160.0 (49.7)	237.5 (53.1)	333.1 (59.9)	228.8 (34.2)	306.0 (63.1)	**1.24**
16	α-phellandrene	Monoterpene	1.2 (0.4)^a	2.0 (0.5)^{ab}	3.1 (0.7)^b	2.3 (0.6)^{ab}	3.7 (1.4)^{ab}	**1.35**
17	(*Z*)-3-hexen-1-ol, acetate	Ester	372.2 (88.1)	747.2 (330.1)	1933.2 (704.1)	444.9 (167.0)	1172.4 (477.7)	0.60
18	hexyl acetate	Ester	17.6 (5.0)	25.4 (8.9)	92.7 (41.7)	14.4 (3.1)	34.8 (13.3)	**1.11**
19	α-terpinene	Monoterpene	19.1 (7.2)^a	32.1 (8.9)^{ab}	50.6 (12.9)^b	37.3 (9.8)^{ab}	59.9 (24.3)^{ab}	**1.40**
20	1,8-cineole	Monoterpene	38.9 (13.1)^a	67.8 (15.3)^{ab}	93.6 (15.3)^b	64.6 (12.2)^{ab}	83.1 (21.1)^{ab}	**1.47**

21	β-isophorone	Ketone	3.8 (0.8)	6.6 (1.5)	3.4 (0.8)	5.7 (3.1)	4.1 (1.0)	0.36
22	(*E*)-β-ocimene	Monoterpene	6.0 (1.6)	7.2 (1.6)	17.9 (6.3)	6.6 (1.2)	12.4 (3.7)	0.20
23	γ-terpinene	Monoterpene	13.8 (4.2)[a]	21.2 (5.0)[ab]	33.0 (7.8)[b]	24.6 (6.3)[ab]	40.4 (14.6)[ab]	**1.23**
24	α-terpinolene	Monoterpene	10.6 (2.9)	15.4 (3.6)	22.8 (4.9)	17.2 (3.3)	28.2 (8.7)	0.31
25	linalool	Monoterpene	7.7 (1.9)	13.2 (6.5)	25.8 (11.3)	5.4 (1.9)	10.4 (3.3)	0.03
26	(*E*)-DMNT	Homoterpene	135.5 (85.2)	126.0 (81.4)	401.3 (178.0)	96.9 (50.9)	104.7 (48.8)	0.71
27	alloocimene	Monoterpene	1.1 (0.3)	1.1 (0.2)	2.1 (0.4)	1.2 (0.3)	1.9 (0.4)	0.70
28	(*Z*)-3-hexen-1-ol, isobutyrate	Ester	1.4 (0.6)	8.2 (5.1)	63.7 (33.7)	2.4 (0.9)	42.7 (26.4)	0.62
29	1-methyl-4-(1-methylethyl) cyclohexanol	Alcohol	73.2 (49.6)	93.6 (70.5)	144.2 (66.5)	91.3 (56.8)	201.6 (83.4)	0.02
30	α-terpineol	Monoterpene	4.4 (1.8)	6.3 (3.9)	7.2 (1.9)	2.4 (0.4)	4.5 (2.1)	0.14
31	(*Z*)-3-hexenyl isovalerate	Ester	5.1 (1.3)	7.3 (3.6)	58.7 (26.0)	4.8 (1.5)	54.0 (44.2)	0.29
32	verbenone	Monoterpene	9.9 (3.0)	5.0 (1.3)	9.3 (4.4)	4.2 (0.6)	5.5 (0.7)	0.51
33	unknown	NA	27.8 (7.9)	13.1 (1.7)	20.4 (8.8)	11.3 (1.7)	17.1 (2.3)	**1.05**
34	isobornyl acetate	Ester	11.7 (2.2)[a]	9.1 (2.6)[ab]	6.8 (2.0)[b]	9.4 (4.0)[ab]	8.1 (2.5)[b]	**1.07**
35	(*Z*)-3-hexen-1-ol, 2-methyl-2-butenoate	Ester	25.6 (4.1)	18.3 (1.9)	36.9 (13.6)	18.3 (3.5)	55.9 (32.7)	0.09
36	unknown	NA	1.3 (0.2)	1.0 (0.1)	1.1 (0.2)	1.0 (0.2)	1.5 (0.2)	0.26
37	isomer of β-elemene	Sesquiterpene	0.3 (0.1)	0.5 (0.4)	1.9 (0.8)	1.2 (0.5)	0.8 (0.5)	0.24
38	β-elemene	Sesquiterpene	4.7 (4.2)	25.2 (18.3)	85.4 (35.8)	61.1 (22.6)	42.1 (25.0)	0.52
39	6,10-dimethyl-2-undecanone	Ketone	21.7 (4.1)	15.2 (2.6)	17.0 (3.5)	16.8 (6.3)	21.9 (3.3)	0.46
40	α-cedrene	Sesquiterpene	6.8 (2.9)	1.2 (0.2)	3.3 (1.4)	1.7 (0.3)	1.4 (0.2)	0.57
41	(*E*)-α-bergamotene	Sesquiterpene	1.2 (0.6)	0.7 (0.5)	2.7 (1.0)	1.9 (0.7)	1.2 (0.7)	0.37
42	(*E*)-β-farnesene	Sesquiterpene	0.3 (0.2)	0.3 (0.1)	1.4 (0.7)	0.6 (0.2)	1.3 (0.9)	0.83
43	β-chamigrene	Sesquiterpene	0.2 (0.1)	0.6 (0.4)	2.3 (1.0)	2.7 (1.2)	1.5 (0.9)	0.65
44	hinesene	Sesquiterpene	0.7 (0.3)[a]	2.1 (0.9)[ab]	8.2 (3.0)[b]	7.5 (3.2)[ab]	5.2 (2.9)[ab]	**1.18**
45	α-zingiberene	Sesquiterpene	0.1 (0.1)	2.3 (1.7)	10.3 (4.9)	4.1 (1.5)	3.6 (2.0)	0.99
46	α-selinene	Sesquiterpene	0.7 (0.4)	2.2 (1.5)	10.3 (4.8)	11.8 (5.5)	7.6 (4.8)	0.03

47	cashmeran	Sesquiterpene	5.7 (2.0)[a]	1.9 (0.2)[b]	3.1 (1.3)[ab]	1.9 (0.3)[b]	2.1 (0.3)[ab]	**1.29**
48	(*E*,*E*)-α-farnesene	Sesquiterpene	11.3 (4.0)	16.7 (6.0)	52.2 (18.6)	20.2 (7.5)	17.3 (5.0)	0.63
49	β-bisabolene	Sesquiterpene	0.5 (0.2)	2.7 (2.2)	9.1 (4.2)	7.3 (2.8)	4.7 (2.8)	0.21
50	(Z)-γ-bisabolene	Sesquiterpene	0.2 (0.2)	1.2 (0.9)	4.0 (1.7)	2.7 (1.0)	1.8 (1.1)	0.90

[x]: Treatments that plants were subjected to: (UD) undamaged control; (S-) ablated *P. brassicae*; (S+) intact *P. brassicae*; (PS-) ablated *Cotesia glomerata*-parasitized *P. brassicae*; (PS+) intact *C. glomerata*-parasitized *P. brassicae.*

Table S2. Summary statistics for labial salivary glands of *Pieris brassicae* transcriptome sequencing and mapping.

	Salivary Glands - unparasitized Larvae	Salivary Glands - Parasitized Larvae
Total number of reads	158 million	161 million
Read length (bases)	100	100
Reads used for TA-contig assembly	90 million	90 million
Reads used for mapping	145 million	147 million
No. of unmapped reads	9.2 million	10.3 million
No. of TA-contigs not covered by read mappings	353	166

Table S3. Contigs with expression ratios greater than 2-fold and P < 0.05 cutoffs in labial salivary glands of unparasitized (PB) or *Cotesia glomerata* parasitized (PB-CG) *Pieris brassicae.*

Name	Seq. Length	Seq. Description	Fold change (PB-CG vs. PB)	P-value
ASS2_C6243	807	hypothetical protein BV9-4	434.046 up	3.49E-08
ASS2_C661	570	bv9 family protein	2713.858 up	3.81E-08
ASS2_C11309	267	---NA---	1697.054 up	3.81E-08
ASS2_C19060	393	---NA---	826.225 up	3.81E-08
ASS2_C7293	495	viral ankyrin	396.114 up	3.81E-08
ASS2_C10750	325	ben domain protein	618.406 up	3.81E-08
ASS2_C17272	736	---NA---	228.266 up	3.81E-08
ASS2_C8771	328	conserved hypothetical protein	595.516 up	3.81E-08
ASS2_C7728	1444	bv6 family protein	2018.533 up	3.81E-08
ASS2_C12266	765	bv21 family protein	465.666 up	3.86E-08
ASS2_C6996	1671	ben domain protein	1576.456 up	4.00E-08
ASS2_C11725	592	host translation inhibitory factor ii	968.504 up	4.00E-08
ASS2_C7673	427	hypothetical protein CcBV_3.3	781.753 up	5.37E-08
ASS2_C14669	272	hypothetical protein BV19-1	248.446 up	7.27E-08
ASS2_C16007	401	viral ankyrin	185.324 up	7.90E-08
ASS2_C8772	377	conserved hypothetical protein	1825.395 up	1.02E-07
ASS2_C1195	938	bv8 family protein	992.447 up	2.15E-07
ASS2_C7326	441	---NA---	278.258 up	4.00E-07
ASS2_C6451	1020	---NA---	572.207 up	4.03E-07
ASS2_C15237	469	---NA---	700.588 up	4.29E-07
ASS2_C22167	240	---NA---	114.425 up	4.87E-07
ASS2_C15618	391	conserved hypothetical ben domain protein	222.547 up	5.31E-07
ASS2_C13627	653	---NA---	333.185 up	5.31E-07
ASS2_C18005	305	elongation factor 1-alpha 1	168.449 up	5.81E-07
ASS2_C18324	476	conserved hypothetical protein	330.481 up	5.81E-07
ASS2_C10675	751	bv6 family protein	573.821 up	6.96E-07
ASS2_C18414	568	ben domain protein	180.534 up	8.25E-07
ASS2_C18393	304	60s ribosomal protein l18	90.335 up	8.77E-07
ASS2_C10616	325	---NA---	339.431 up	1.27E-06
ASS2_C16839	609	---NA---	209.063 up	1.33E-06
ASS2_C19247	330	40s ribosomal protein s3a	163.773 up	1.35E-06
ASS2_C15189	801	serine proteinase stubble-like	291.707 up	1.35E-06
ASS2_C1718	3268	ben domain protein	2213.795 up	1.36E-06
ASS2_C14161	322	---NA---	122.092 up	1.36E-06
ASS2_C21768	222	---NA---	190.295 up	1.48E-06
ASS2_C21673	408	arylphorin subunit alpha	140.987 up	1.57E-06
ASS2_C19831	243	elongation factor 1 partial	227.771 up	1.73E-06
ASS2_C14624	284	elongation factor 1- partial	258.977 up	1.82E-06
ASS2_C14301	317	conserved hypothetical ben domain protein	169.293 up	3.06E-06
ASS2_C21746	253	protein disulfide-isomerase a6	145.178 up	3.42E-06
ASS2_C18018	356	protein disulfide-isomerase a3	136.833 up	3.53E-06
ASS2_C23282	296	Hexamerin	136.362 up	4.15E-06
ASS2_C16515	288	---NA---	111.581 up	4.38E-06
ASS2_C17856	763	arylphorin subunit alpha	188.305 up	4.41E-06
ASS2_C18848	213	conserved hypothetical ben domain protein	164.110 up	4.99E-06
ASS2_C13830	273	conserved hypothetical ben domain protein	205.254 up	5.20E-06
ASS2_C5956	205	---NA---	1686.710 up	7.27E-06
ASS2_C15682	521	heat shock 70 kda protein cognate 3	291.209 up	7.27E-06

ASS2_C7462	622	ben domain protein	190.488 up	8.85E-06
ASS2_C18758	270	atp-dependent rna helicase	456.282 up	9.28E-06
ASS2_C22276	303	---NA---	72.078 up	1.01E-05
ASS2_C21636	281	beta-glucosidase precursor	117.647 up	1.04E-05
ASS2_C22308	234	ribosomal protein l21	91.838 up	1.36E-05
ASS2_C555	825	hypothetical protein CcBV_26.4	1286.045 up	1.56E-05
ASS2_C4762	243	---NA---	159.196 up	1.86E-05
ASS2_C13012	540	---NA---	247.138 up	1.86E-05
ASS2_C12220	463	---NA---	609.757 up	1.92E-05
ASS2_C22211	261	---NA---	155.129 up	2.09E-05
ASS2_C12750	524	conserved hypothetical ben domain protein	150.053 up	2.22E-05
ASS2_C14901	339	hypothetical protein 32.18	96.336 up	2.47E-05
ASS2_C17042	284	conserved hypothetical ben domain protein	81.312 up	2.97E-05
ASS2_C13786	221	---NA---	200.294 up	3.28E-05
ASS2_C4390	964	ben domain protein	274.449 up	4.12E-05
ASS2_C19222	229	---NA---	113.415 up	4.12E-05
ASS2_C17335	246	---NA---	149.309 up	4.12E-05
ASS2_C12779	287	dihydrolipoyllysine-residue acetyltransferase component 2 of pyruvate dehydrogenase mitochondrial isoform x1	145.864 up	4.15E-05
ASS2_C12510	312	Hexamerin	235.745 up	4.25E-05
ASS2_C12927	823	protein disulfide-isomerase a6	168.380 up	4.61E-05
ASS2_C17285	244	---NA---	203.201 up	4.61E-05
ASS2_C20939	276	---NA---	87.571 up	4.61E-05
ASS2_C23568	426	arylphorin subunit alpha	163.075 up	4.71E-05
ASS2_C15242	402	conserved hypothetical ben domain protein	154.628 up	4.71E-05
ASS2_C11672	401	ep1-like protein	152.750 up	4.97E-05
ASS2_C16786	324	ben domain protein	117.949 up	5.33E-05
ASS2_C13301	291	---NA---	160.661 up	8.24E-05
ASS2_C9775	1201	ben domain protein	1622.121 up	8.45E-05
ASS2_C21223	220	---NA---	59.027 up	8.94E-05
ASS2_C15856	520	protein npc2 homolog	137.412 up	9.42E-05
ASS2_C14303	437	ben domain protein	102.217 up	0.000104
ASS2_C10688	311	---NA---	116.212 up	0.000133
ASS2_C14871	1304	bv21 family protein	37.601 up	0.000148
ASS2_C4186	3227	melanization-related protein	1075.936 up	0.000165
ASS2_C2834	2020	arylsulfatase b	8.706 up	0.000175
ASS2_C17017	409	---NA---	97.246 up	0.000198
ASS2_C21156	327	hexamerin-like	94.453 up	0.000202
ASS2_C9953	344	hypothetical protein BV22-2	100.131 up	0.000227
ASS2_C20401	391	protein npc2 homolog	194.104 up	0.000263
ASS2_C6063	1052	protein tyrosine phosphatase	650.031 up	0.00031
ASS2_C7025	646	bv6 family protein	3322.083 up	0.000317
ASS2_C17723	232	aminopeptidase n	73.666 up	0.000366
ASS2_C5385	1275	bv8 family protein	1123.172 up	0.000429
ASS2_C12039	649	hypothetical protein CcBV_19.4	150.399 up	0.000472
ASS2_C16807	344	---NA---	86.837 up	0.000474
ASS2_C17992	396	serine carboxypeptidase precursor family protein	75.434 up	0.00053
ASS2_C9212	838	---NA---	708.745 up	0.00056
ASS2_C11871	467	transmembrane and tpr repeat-containing protein 1-like	7.996 up	0.000691
ASS2_C23037	419	histone h2b	116.479 up	0.000713
ASS2_C22179	275	---NA---	65.713 up	0.000774
ASS2_C5135	3044	rna-directed dna polymerase from mobile element jockey-like	813.902 up	0.000787

ASS2_C17404	268	---NA---	2.531 up	0.000795
ASS2_C12820	967	ser-rich protein	435.474 up	0.000797
ASS2_C906	2344	ben domain protein	769.345 up	0.000804
ASS2_C4656	785	leucine-rich repeat-containing protein ddb_g0290503-like	4.397 up	0.000804
ASS2_C19360	241	hypothetical protein CAPTEDRAFT_206368	113.950 up	0.000864
ASS2_C19170	237	conserved hypothetical protein	97.438 up	0.00095
ASS2_C1396	1784	cytochrome p450	3.009 up	0.000961
ASS2_C2927	1266	viral ankyrin	2703.799 up	0.00102
ASS2_C21731	274	60s ribosomal protein l5	74.936 up	0.00102
ASS2_C10328	1016	Calreticulin	240.053 up	0.00107
ASS2_C2748	2973	glucose dehydrogenase	2.451 up	0.00115
ASS2_C18686	248	---NA---	97.458 up	0.00122
ASS2_C2579	1545	alpha-tocopherol transfer	2.811 up	0.00128
ASS2_C16634	460	---NA---	8.862 up	0.00129
ASS2_C22056	237	ep1-like protein	169.234 up	0.00159
ASS2_C21726	263	---NA---	72.572 up	0.00177
ASS2_C4389	2901	ben domain protein	492.251 up	0.00179
ASS2_C17835	259	coatomer subunit partial	68.579 up	0.00182
ASS2_C12167	650	neutral endopeptidase	4.225 up	0.00212
ASS2_C6402	825	---NA---	1393.452 up	0.00224
ASS2_C3259	1718	aromatic-l-amino-acid decarboxylase-like	3.517 up	0.00252
ASS2_C16516	339	60s ribosomal protein l18a	65.883 up	0.0027
ASS2_C6329	1107	hydroxybutyrate dehydrogenase	2.645 up	0.0027
ASS2_C19889	241	---NA---	43.291 up	0.00318
ASS2_C9865	1685	---NA---	3.393 up	0.00324
ASS2_C18866	279	hypothetical protein KGM_00511	46.544 up	0.00347
ASS2_C5370	211	---NA---	2371.357 up	0.00377
ASS2_C3834	2228	nucleolar complex protein 2 homolog	2.196 up	0.00397
ASS2_C19955	290	---NA---	3.617 up	0.0042
ASS2_C15755	350	ben domain protein	73.914 up	0.0046
ASS2_C4199	204	---NA---	4.251 up	0.00485
ASS2_C22720	325	hypotetical protein bv4-1	67.888 up	0.00497
ASS2_C6596	2538	facilitated trehalose transporter tret1-like	2.878 up	0.00581
ASS2_C5206	3998	thrombospondin type-1 domain-containing protein 7a	2.028 up	0.00602
ASS2_C16852	276	histone h4	81.869 up	0.00606
ASS2_C6876	3280	2-oxoglutarate dehydrogenase	2.317 up	0.00644
ASS2_C10997	531	von willebrand factor d and egf domain-containing protein	3.282 up	0.00644
ASS2_C13051	201	---NA---	1149.161 up	0.00672
ASS2_C553	1349	heat shock 70 kda protein cognate 3 isoform x1	108.024 up	0.00681
ASS2_C9660	659	bv9 family protein	142.869 up	0.00735
ASS2_C3009	374	cg10200	3.222 up	0.00742
ASS2_C18001	355	---NA---	123.121 up	0.00787
ASS2_C14542	356	ubiquitin-activating enzyme e1	67.892 up	0.00828
ASS2_C6446	1390	facilitated trehalose transporter tret1-like	3.362 up	0.00828
ASS2_C16830	512	retrovirus-related pol polyprotein from transposon 412	7.828 up	0.00828
ASS2_C6652	651	apolipoprotein d-like isoform x2	337.219 up	0.00842
ASS2_C9184	3112	disintegrin and metalloproteinase domain-containing protein 12-like	3.399 up	0.00881
ASS2_C2404	750	ben domain protein	448.924 up	0.0101
ASS2_C14310	858	---NA---	2.569 up	0.0106
ASS2_C19055	293	cytochrome p450	5.070 up	0.0107

ASS2_C4550	357	ornithine decarboxylase	2.966 up	0.0111
ASS2_C262	2528	heat shock protein 90	2.201 up	0.0111
ASS2_C6635	1135	ben domain protein	95.765 up	0.0117
ASS2_C12660	708	ecdysone-inducible protein partial	4.549 up	0.0117
ASS2_C17829	1283	ovalbumin-related protein x isoform x12	98.484 up	0.0117
ASS2_C12102	789	ben domain protein	191.869 up	0.0128
ASS2_C19713	388	neurotransmitter gated ion channel	7.291 up	0.0132
ASS2_C10039	330	---NA---	2.728 up	0.0133
ASS2_C11872	821	beta lysosomal	3.660 up	0.0133
ASS2_C9654	757	lysozyme-like	2.148 up	0.0136
ASS2_C1949	1619	sucrose-6-phosphate hydrolase	2.141 up	0.0138
ASS2_C890	568	cuticle protein cpg43	2.042 up	0.014
ASS2_C18418	295	---NA---	2.477 up	0.015
ASS2_C12797	1135	glycerophosphoryl diester periplasmic	3.883 up	0.015
ASS2_C9803	207	---NA---	2.821 up	0.0154
ASS2_C3326	1332	apolipoprotein d	2.694 up	0.0154
ASS2_C14371	473	ben domain protein	98.277 up	0.0159
ASS2_C10930	1276	hypothetical protein KGM_08735	2.209 up	0.0161
ASS2_C12603	780	atp synthase subunit mitochondrial-like	5.542 up	0.0162
ASS2_C9754	1738	cysteine synthase	2.053 up	0.0168
ASS2_C4142	245	---NA---	3.002 up	0.0169
ASS2_C12843	265	hypothetical protein KGM_04641	2.355 up	0.0174
ASS2_C11363	456	---NA---	7.800 up	0.0176
ASS2_C14682	1812	mind- isoform b	4.189 up	0.0176
ASS2_C17144	407	---NA---	110.267 up	0.0195
ASS2_C7818	1085	arylalkylamine n-acetyltransferase	2.983 up	0.0195
ASS2_C2740	316	alpha amylase	2.445 up	0.0199
ASS2_C14422	388	---NA---	2.111 up	0.0202
ASS2_C15995	471	---NA---	3.655 up	0.0203
ASS2_C15455	284	---NA---	2.800 up	0.0212
ASS2_C6991	1437	glycine n-methyltransferase-like	2.609 up	0.0213
ASS2_C8823	378	---NA---	3.199 up	0.0221
ASS2_C9164	943	inosine-uridine preferring nucleoside hydrolase	3.187 up	0.0222
ASS2_C6324	1165	aldose 1-epimerase	2.269 up	0.0234
ASS2_C4454	892	hypothetical protein KGM_07240	2.716 up	0.0248
ASS2_C22586	360	cytosolic carboxypeptidase -like	5.212 up	0.0257
ASS2_C20233	599	---NA---	50.638 up	0.0259
ASS2_C7559	1656	organic cation transporter	2.892 up	0.026
ASS2_C7800	462	igf2 mrna binding protein	2.131 up	0.026
ASS2_C20012	423	aldehyde dehydrogenase family 1 member l1-like isoform 1	2.802 up	0.0261
ASS2_C23238	395	elongation of very long chain fatty acids protein 4	54.100 up	0.0264
ASS2_C18901	378	---NA---	2.416 up	0.0266
ASS2_C3051	679	---NA---	2.817 up	0.0271
ASS2_C6162	268	---NA---	2.257 up	0.0272
ASS2_C5771	255	---NA---	3.147 up	0.0273
ASS2_C5644	1122	calcitonin receptor	2.047 up	0.0275
ASS2_C18143	247	---NA---	2.645 up	0.0278
ASS2_C9198	883	elongation of very long chain fatty acids protein 4	2.110 up	0.0286
ASS2_C20174	475	PREDICTED: uncharacterized protein LOC101736715	4.707 up	0.0294
ASS2_C674	1483	neurofilament heavy polypeptide-like isoform x2	2.049 up	0.0297
ASS2_C20479	276	zinc finger protein 177-like	2.375 up	0.0303
ASS2_C11207	246	---NA---	3.145 up	0.0303
ASS2_C1153	2228	nucleolar protein 66	2.315 up	0.0305

ASS2_C8534	447	armadillo repeat-containing protein 3-like	3.473 up	0.0308
ASS2_C18280	639	membrane metallo-endopeptidase-like 1-like	2.384 up	0.0314
ASS2_C10540	586	hypothetical protein CcBV_28.4	63.045 up	0.0321
ASS2_C14407	651	isoform c	2.444 up	0.034
ASS2_C18749	560	organic cation transporter	4.761 up	0.0342
ASS2_C16763	274	---NA---	2.460 up	0.0346
ASS2_C16235	344	transcription factor e75a	3.247 up	0.0356
ASS2_C18400	520	isoform f	3.404 up	0.0361
ASS2_C8032	329	hypothetical protein KGM_17951	2.743 up	0.0382
ASS2_C6744	530	cg10035-pa	4.866 up	0.0382
ASS2_C14585	390	cytoplasmic polyadenylation element-binding protein 1-like	4.233 up	0.0385
ASS2_C20382	291	bv6 family protein	62.058 up	0.039
ASS2_C8861	256	---NA---	2.049 up	0.0391
ASS2_C8860	1655	kruppel homolog 1	43.687 up	0.0417
ASS2_C14356	941	zinc finger protein	2.000 up	0.0423
ASS2_C8363	283	---NA---	2.484 up	0.0431
ASS2_C18313	438	hypothetical protein TcasGA2_TC002700	42.344 up	0.0431
ASS2_C15012	623	btb poz domain-containing protein kctd1-like	4.273 up	0.0433
ASS2_C18584	563	---NA---	2.457 up	0.0433
ASS2_C18556	532	isoform c	2.585 up	0.0446
ASS2_C10040	872	sarcoplasmic calcium-binding	2.765 up	0.0452
ASS2_C21175	396	transmembrane and tpr repeat-containing protein 1-like	2.311 up	0.0456
ASS2_C16709	386	---NA---	3.393 up	0.0462
ASS2_C10828	774	PREDICTED: uncharacterized protein LOC101741240	3.138 up	0.0473
ASS2_C4132	542	acyl- z9 desaturase	3.030 up	0.0473
ASS2_C17441	317	---NA---	5.155 up	0.0475
ASS2_C14433	1052	cuticular protein analogous to peritrophins 1-g	2.034 up	0.0475
ASS2_C1185	1146	PREDICTED: uncharacterized protein LOC101741030	2.321 up	0.0476
ASS2_C17735	467	isoform a	3.955 up	0.0481
ASS2_C4686	1624	venom acid phosphatase acph-1-like	2.183 up	0.0482
ASS2_C11385	209	---NA---	2.101 up	0.0482
ASS2_C13136	622	pdz and lim domain protein 3-like	3.187 up	0.0488
ASS2_C3752	1388	trehalase- partial	8.482 up	0.0491
ASS2_C17278	595	---NA---	3.195 up	0.0492
ASS2_C6256	1506	leucine zipper tumor suppressor 2 homolog	2.076 up	0.0492
ASS2_C22389	402	---NA---	2.171 down	0.05
ASS2_C15400	329	---NA---	3.548 down	0.0493
ASS2_C23944	326	takeout jhbp like protein	57.415 down	0.0492
ASS2_C15079	486	---NA---	2.259 down	0.0492
ASS2_C16598	418	---NA---	2.236 down	0.0484
ASS2_C20434	434	isoform c	5.047 down	0.0483
ASS2_C17284	393	---NA---	2.254 down	0.0482
ASS2_C20893	264	calbindin-32 isoform x2	2.777 down	0.0475
ASS2_C13815	775	integrase core domain protein	2.079 down	0.0469
ASS2_C13756	637	monocarboxylate transporter	3.344 down	0.0469
ASS2_C22905	344	interferon gamma induced gtpase	4.192 down	0.0466
ASS2_C16876	665	---NA---	2.131 down	0.0443
ASS2_C14032	292	PREDICTED: uncharacterized protein LOC101743931	2.028 down	0.0443
ASS2_C21068	417	endonuclease and reverse transcriptase-like protein	2.188 down	0.0443
ASS2_C18160	314	---NA---	2.121 down	0.0441
ASS2_C13537	857	latrophilin-like receptor	2.308 down	0.0436
ASS2_C16866	554	---NA---	3.046 down	0.0436
ASS2_C15978	528	---NA---	2.502 down	0.0436

ASS2_C23861	239	non-ltr retrotransposon cats	75.556 down	0.0435
ASS2_C21827	283	---NA---	2.955 down	0.0431
ASS2_C7737	799	---NA---	2.152 down	0.0431
ASS2_C13465	773	---NA---	2.499 down	0.0431
ASS2_C18815	406	---NA---	2.422 down	0.0423
ASS2_C17655	329	---NA---	2.878 down	0.0423
ASS2_C23434	275	---NA---	5.704 down	0.0415
ASS2_C15835	427	---NA---	2.344 down	0.0412
ASS2_C9788	1184	---NA---	2.038 down	0.0404
ASS2_C19374	337	eukaryotic peptide chain release factor subunit 1-like isoform	2.256 down	0.0401
ASS2_C21090	456	---NA---	2.096 down	0.04
ASS2_C16061	559	---NA---	2.152 down	0.0398
ASS2_C10171	1776	hypothetical protein KGM_22069	2.657 down	0.0386
ASS2_C17795	348	---NA---	3.447 down	0.0385
ASS2_C10175	295	---NA---	2.420 down	0.0378
ASS2_C22330	359	---NA---	2.059 down	0.0369
ASS2_C3899	637	uncharacterized atp-dependent helicase yhr031c	2.576 down	0.0368
ASS2_C20792	520	larval cuticle protein lcp-17-like	9.364 down	0.0363
ASS2_C15062	682	---NA---	7.235 down	0.0358
ASS2_C15285	383	---NA---	2.378 down	0.0356
ASS2_C20078	559	heat shock protein	2.739 down	0.0356
ASS2_C7679	1639	reverse transcriptase	2.393 down	0.0356
ASS2_C1968	1866	repeat element protein-	2.293 down	0.0354
ASS2_C9689	432	---NA---	2.176 down	0.0345
ASS2_C19022	524	---NA---	2.816 down	0.0344
ASS2_C12420	306	---NA---	2.927 down	0.0342
ASS2_C15150	1048	---NA---	2.052 down	0.0337
ASS2_C12333	829	---NA---	2.536 down	0.0327
ASS2_C18472	1701	nephrin isoform x1	6.635 down	0.0304
ASS2_C15308	1080	hypothetical protein KGM_00708	2.753 down	0.0304
ASS2_C16540	456	hypothetical protein KGM_10651	3.111 down	0.0299
ASS2_C16106	657	---NA---	2.577 down	0.0299
ASS2_C13987	827	prophenoloxidase subunit 1	2.057 down	0.0295
ASS2_C18595	404	orphan nuclear receptor e75c	6.300 down	0.0291
ASS2_C6557	662	---NA---	2.042 down	0.0271
ASS2_C22571	242	zinc finger protein 271 (zinc finger protein 7) (zinc finger protein znfphex133) (epstein-barr virus-induced zinc finger protein) (znf-eb) (ct-zfp48) (zinc finger protein	4.583 down	0.0271
ASS2_C17270	1058	---NA---	3.063 down	0.026
ASS2_C6089	394	---NA---	2.067 down	0.0257
ASS2_C12619	389	---NA---	2.839 down	0.0256
ASS2_C13101	1488	protein takeout-like	3.745 down	0.0248
ASS2_C9311	750	PREDICTED: uncharacterized protein LOC101746304	4.712 down	0.0243
ASS2_C21973	497	storage protein 1	98.721 down	0.0243
ASS2_C12643	782	polypeptide n-acetylgalactosaminyltransferase 9-like isoform	2.277 down	0.0237
ASS2_C19871	374	mutant cadherin	3.622 down	0.0234
ASS2_C17798	447	---NA---	3.323 down	0.0227
ASS2_C11419	241	---NA---	2.086 down	0.0222
ASS2_C9045	507	wd repeat-containing protein 81	2.006 down	0.0222
ASS2_C20089	519	---NA---	2.188 down	0.0212
ASS2_C15414	1427	---NA---	2.024 down	0.0211

ASS2_C17473	812	---NA---	2.843 down	0.0203
ASS2_C10757	845	protein cubitus interruptus	2.397 down	0.0202
ASS2_C20296	456	---NA---	2.515 down	0.0199
ASS2_C17003	412	nesprin-1-like isoform x2	2.209 down	0.0195
ASS2_C11371	1150	---NA---	2.409 down	0.0187
ASS2_C9753	831	---NA---	2.423 down	0.0185
ASS2_C17413	664	nascent polypeptide-associated complex subunit muscle-specific form-like	2.187 down	0.0176
ASS2_C13534	488	---NA---	3.955 down	0.017
ASS2_C875	521	---NA---	2.803 down	0.0154
ASS2_C23936	472	cuticular protein rr-1 motif 46	190.735 down	0.015
ASS2_C20818	2329	moderately methionine rich storage protein	333.589 down	0.014
ASS2_C4875	2749	PREDICTED: uncharacterized protein LOC763787	3.495 down	0.014
ASS2_C5226	322	---NA---	3.980 down	0.0139
ASS2_C1770	4544	low quality protein: supervillin-like	2.079 down	0.0134
ASS2_C2451	550	---NA---	2.187 down	0.0132
ASS2_C7853	1974	---NA---	2.856 down	0.0124
ASS2_C15020	816	---NA---	2.664 down	0.0119
ASS2_C17614	565	hypothetical protein KGM_17409	4.525 down	0.0117
ASS2_C20696	2360	moderately methionine rich storage protein	168.850 down	0.011
ASS2_C7841	1038	calbindin-32-like isoform x1	2.381 down	0.00964
ASS2_C6231	1071	repeat element protein-	2.352 down	0.00961
ASS2_C21583	270	---NA---	2.141 down	0.00938
ASS2_C16717	924	sodium channel protein type 7 subunit alpha	2.130 down	0.00932
ASS2_C15229	493	---NA---	3.154 down	0.00932
ASS2_C11171	531	hypothetical protein KGM_13152	3.309 down	0.00881
ASS2_C2519	3462	breast carcinoma amplified sequence	2.043 down	0.00741
ASS2_C23934	820	tpa: cuticle protein	37.879 down	0.00722
ASS2_C23995	226	---NA---	71.899 down	0.00651
ASS2_C4190	882	calbindin-32-like isoform x2	2.669 down	0.00627
ASS2_C23972	399	27 kda hemolymph protein	87.795 down	0.00602
ASS2_C19283	556	---NA---	3.319 down	0.00493
ASS2_C18134	2059	gpi-anchor transamidase	4.063 down	0.00485
ASS2_C11852	2748	protein distal antenna	3.435 down	0.00481
ASS2_C3180	2932	beta-glucosidase precursor	2.136 down	0.0035
ASS2_C11784	499	---NA---	3.614 down	0.0027
ASS2_C13030	1786	e3 ubiquitin-protein ligase protein pff1365c-like	5.120 down	0.00261
ASS2_C17564	296	---NA---	3.433 down	0.00208
ASS2_C5191	2220	arylphorin precursor	126.401 down	0.00146
ASS2_C1911	2688	isoform d	3.480 down	0.00142
ASS2_C20725	2325	methionine-rich storage protein	102.093 down	0.000474
ASS2_C23935	1382	arylphorin subunit alpha	231.013 down	0.000264
ASS2_C23991	233	---NA---	112.060 down	3.58E-05
ASS2_C23974	253	---NA---	202.078 down	7.30E-06